Annali di Matematica pura ed applicata
(IV), Vol. CLXXIV (1998), pp. 121-134

The Multiple-Scale Transport Equation in One Space Dimension (*) (**).

L. G. DE PILLIS

Abstract. – *This study examines the behavior of the one-dimensional non-homogeneous transport equation of the form $\varepsilon u_t = u_x + f$, $\varepsilon \ll 1$. The solution consists of behavior which changes on two different time scales, one rapid and one slow. This time scale behavior is known. Additionally, however, we find here that because of the presence of the non-homogeneous forcing term f, and large wave speed $1/\varepsilon$, there is a component of the solution which will vary only on a very large* spatial *scale. This large space-scale solution persists throughout all time, even after the source term of the solution has been shut off. The analysis of this large space-scale behavior is the focus of this paper. Numerical experiments highlight some of our results. These results have applications in fields such as meteorology, and other areas where multiple time scales are of interest.*

1. – Introduction.

In the process of modeling certain interesting physical phenomena, such as sound propagation, the equations that often arise are the well-known Navier-Stokes equations of fluid flow; in particular, one makes use of the slightly compressible Navier-Stokes equations when dealing with acoustical problems. It has been shown in [3] how the slightly compressible Navier-Stokes equations in an infinite plane will transition to the wave equation for the pressure in the far-field. Related work can be found in [5] and [10]. If one is eventully to exploit this fact in computation, we must make a more thorough study of the wave equation which arises. The Cauchy problem for the wave equation is given by

$$(1) \qquad \begin{cases} \varepsilon^2 u_{tt}(\boldsymbol{x}, t) = \Delta u(\boldsymbol{x}, t) + f(\boldsymbol{x}, t), & t \geqslant 0\,, \\ u(\boldsymbol{x}, 0) = u_0(\boldsymbol{x})\,, \\ u_t(\boldsymbol{x}, 0) = u_1(\boldsymbol{x}) \end{cases}$$

(*) Entrata in Redazione il 21 novembre 1995 e, in versione riveduta il 3 maggio 1996.
Indirizzo dell'A.: Department of Mathematics, Harvey Mudd College, Claremont, CA 91711, USA.
(**) This work was supported in part by NSF grant NSF-DMS93-21728.

where $1/\varepsilon \gg 1$ is the constant wave speed, $\boldsymbol{x} = (x_1, \ldots, x_n)$ is a point in real n-dimensional Euclidean space, and u, u_0, u_1, $f \in C^\infty$ are scalar valued functions. The forcing function f and the initial data u_0 and $\int u_1 \, d\boldsymbol{x}$ are assumed to have compact support in space.

The analysis in this work will be confined to one space dimension. Extensions to higher dimensions will be forthcoming in later works. We note that in one space dimension, the wave equation can be written as a decoupled system of first order (trasport) equations, cf. [9]. Since the system can be decoupled, the wave equation case is reduced to that of the transport equation. We study, therefore, the behavior of the Cauchy problem for the non-homogeneous transport equation, on an infinite domain, of the form

$$\begin{cases} \varepsilon u_t = u_x + f(x, t), & x \in \mathcal{R}^1, \quad t \geq 0, \\ u(x, 0) = u_0(x), & x \in \mathcal{R}^1 \end{cases} \tag{2}$$

where u, u_0 and f are as described above.

An analysis can also be carried out on a periodic domain, and would be similar to that of the infinite domain in many respects. There are, however, some significant differences in the behavior of the periodic versus infinite solutions. On a periodic domain, standard asymptotic expansion of the transport equation solution will be uniformly valid. Fast parts of the solution will arise from non-zero initial data, and these fast waves will remain in the domain of interest for all time. On an infinite domain, however, an asymptotic expansion of the solution will only be valid if the initial data and the forcing function decay rapidly enough in space so that the solution of the transport equation is bounded. We note that the solution of the transport equation on and infinite domain can be shown to be bounded in terms of the L_2 norms of the initial data and the forcing function, cf. [9].

We will show that on an infinite domain, the presence of the forcing function $f(x, t)$, in conjunction with large wave speed $1/\varepsilon \gg 1$, gives rise to large space scale waves, which persist in time, even after the forcing function has been shut off. On a periodic domain, however, where the period $L \ll 1/\varepsilon$, the large space scale waves will not be observable. Stated formally, we have

THEOREM 1. – *Let function $f(x, t)$ be compact in space (x) and in time (t), and be differentiable to at least order p in space and time. Then the solution of the Cauchy problem given in* (2) *can be expressed as*

$$u(x, t) = u_0(x + t/\varepsilon) + S_0(x + t/\varepsilon) + S(x, t) + Q(\varepsilon x, t) + \mathcal{O}(\varepsilon^p) \tag{3}$$

where u_0 is the compact initial data function. It also follows that S_0 is bounded by $\mathcal{O}(1/x)$ behavior in space. $S(x, t)$ is bounded by the behavior of the high frequency portion of the forcing function $f(x, t)$ and its derivatives. $Q(x, t)$, the large scale component of the solution, persists in time, even after the forcing function has decayed away in time.

In Section 2, we give the proof of this theorem. In Section 3 we present some numerical experiments which illustrate the low and high frequency behavior predicted by the theory.

Equation (2) is of interest in problems corresponding to waves with large wave speed, including electromagnetism, acoustics and meteorology, where in certain applications, the forcing function introduces long waves into a system. It has been observed that in some cases, these long waves remain even after the source of the waves has been shut off. An understanding of the causes for this behavior can be enhanced through the mathematical analysis of this simple transport equation.

2. – The first order wave equation in one dimension.

We begin our analysis by examining the first order one-dimensional one-way wave equation, or transport equation, on an infinite domain, of the form

$$\begin{cases} \varepsilon u_t(x, t) = u_x(x, t) + \underbrace{f(x, t)}_{\text{Forcing function}}, & x \in \mathcal{R}^1, \quad t \geq 0, \\ u(x, 0) = u_0(x), & x \in \mathcal{R}^1, \end{cases} \tag{4}$$

Functions u_0 and $f(x, t)$ are C^∞ and compact in space. Function $f(x, t)$ is also C^∞ and compact in time. The exact solution of equation (4) is well known and is given by

$$u(x, t) = u_0\left(x + \frac{1}{\varepsilon}t\right) + \frac{1}{\varepsilon}\int_0^1 f\left(x + \frac{1}{\varepsilon}t - \frac{1}{\varepsilon}\tau, \tau\right) d\tau . \tag{5}$$

The solution (5) has components which vary on time scales of $\mathcal{O}(t)$ (slow) and $\mathcal{O}(t/\varepsilon)$ (fast). The proof of the existence of two time scales in equations of the form of equation (4), in addition to equations of more general form, is given in great detail in [6, 7, 8]. In meteorological as well as other applications, one is often interested in the portion of these solutions which varies on the slow time scale only. This is because it is generally on this time scale that interesting qualitative behavior of physical phenomena, such as weather systems, evidences itself. It has been shown in [7] as well as in [8] that the Bounded Derivative Principle is valid for equations of this type. (See also [2] for a description of the Bounded Derivative Principle as applied to nonlinear equations.) The Bounded Derivative Principle for partial differential equations is stated in [7] as follows:

THEOREM 2. – *Assume that p time derivatives at $t = 0$ are bounded independently of ε. Then the same is true in a time interval $0 \leq t \leq T$, where $T > 0$ does not depend on ε.*

A proof of the Bounded Derivative Principle is also provided by KREISS in [7], so we do not include it here. The implications of the Bounded Derivative Principle are given in detail in the above references. One of the implicaions which is discussed at length in [6, 7, 8] is that by the Bounded Derivative Principle, one can choose the initial data

$u_0(x)$ so that within a finite time interval, rapid time oscillations in the solution u, and its derivative up to a certain order, will not be excited. Therefore, according to the work in [2] and in [6, 7, 8], if the initial data are properly chosen, they will have a negligible effect on the solution within a finite time interval.

It is easily seen by (5) that general initial data move at speed $\mathcal{O}(t/\varepsilon)$ through the domain of observation. Localized initial data will continue to have a localized effect on the overall solution throughout time, and will eventually be transported out of the domain of observation. The solution form of (5), however, does not immediately evidence the remaining elements of the solution described in Theorem 1. In order to find these, we carry out our analysis in frequency space through Fourier transforms.

We define the Fourier transform pair to be given by

$$f(x, t) = \frac{1}{\sqrt{2\pi}} \int_{-\infty} e^{ix\xi} \hat{f}(\xi, t)\, d\xi\,, \qquad \hat{f}(\xi, t) = \frac{1}{\sqrt{2\pi}} \int_{-\infty} e^{ix\xi} f(x, t)\, d\xi\,. \tag{6}$$

It is clear that the function $\hat{f}(\xi, t)$ is bounded in ξ since $f(x, t)$ is compactly supported in space. This would also be the case had we only specified that $f(x, t)$ decay rapidly to zero for large x, as opposed to having specifically compact support. In fact, standard Fourier theory tells us that the faster the decay rate of f as $|x| \to \infty$, the smoother $\hat{f}(\xi, t)$ is; similarly, the faster $\hat{f}(\xi, t)$ decays as $|\xi| \to \infty$, the smoother $f(x, t)$ is. The derivatives of all orders of $\hat{f}$ decay to zero for large ξ as rapidly as is necessary for our analysis. Clearly, the inverse Fourier transforms of $\hat{f}(\xi, t)$ and all derivatives of $\hat{f}(\xi, t)$ exist.

Let us define cut-off function χ to be the step function

$$\chi(\xi) = \begin{cases} 1 & \text{for } |\xi| \le \eta\,, \\ 0 & \text{for } |\xi| > \eta\,. \end{cases} \tag{7}$$

We can then describe our Fourier transformed forcing function $\hat{f}$ by $\hat{f} = \hat{f}_1 + \hat{f}_2$ where

$$\hat{f}_1 = \chi \hat{f}\,, \qquad \text{and } \hat{f}_2 = (1 - \chi)\, \hat{f}\,. \tag{8}$$

Both $\hat{f}_1$ and $\hat{f}_2$ are bounded in ξ, since $\hat{f}$ itself is bounded in ξ. By the definitions, both $\hat{f}_1$ and $\hat{f}_2$ are piecewise smooth, containing only a finite number of jump discontinuities. According to standard Fourier theory (cf. [1]), this implies that the inverse transforms, $f_1(x, t)$ and $f_2(x, t)$, will decay in physical space at least as rapidly as $1/x$ for large x. Additionally, both $f_1(x, t)$ and $f_2(x, t)$ are bounded over all x. Had we chosen the cut-off function χ to be smoother than a step function, then the $\hat{f}_j(x, t)$, $j = 1, 2$, would have been smoother, making the decay of $f_j(x, t)$ in physical space more rapid. For our purposes, however, inverse distance decay is sufficient.

We now write the Fourier transform of $u(x, t)$ as a sum of two functions, $\hat{u}(\xi, t) = \hat{v}(\xi, t) + \hat{w}(\xi, t)$, where $\hat{w}$ satisfies

$$\begin{cases} \varepsilon \hat{w}_t(\xi, t) = i\varepsilon \hat{w}(\xi, t) + \hat{f}_2(\xi, t)\,, \\ \hat{w}(\xi, 0) = \hat{u}_0(\xi)\,, \end{cases} \tag{9}$$

and $\widehat{v}$ satisfies

$$\begin{cases} \varepsilon\widehat{v}_t(\xi, t) = i\varepsilon\widehat{v}(\xi, t) + \hat{f}_1(\xi, t), \\ \widehat{v}(\xi, 0) = 0. \end{cases} \tag{10}$$

In the next sections, we examine solutions $\widehat{v}$ and $\widehat{w}$ arising from the respective forcing functions $\hat{f}_1$ and $\hat{f}_2$. We keep in mind that f_1 is the inverse transform of $\hat{f}_1$, which has supporte *over* an η-neighborhood of the origin, and f_2 is the inverse transform of $\hat{f}_2$, which has support *outside* an η-neighborhood of the origin. The question arises as to how to choose η appropriately. This will be determined upon examining solution $\widehat{v}$ and $\widehat{w}$.

2.1. *High frequency driven behavior.*

Let us first examine the behavior of the solution w to equation (9). An asymptotically expanded representation of the solution $\widehat{w}$ is achieved by following the method outlined in [6]. The expanded solution to (9) is then given by

$$\widehat{w} = -\sum_{j=0}^{p-1} \frac{\varepsilon^j}{(i\xi)^{j+1}} \frac{\partial^j \hat{f}_2(\xi, t)}{\partial t^j} + \widehat{w}_p = \widehat{S} + \widehat{w}_p \tag{11}$$

where $\widehat{S}$ is the Fourier transformed forcing driven slow part of the solution, and where the remainder term $\widehat{w}_p$ is described by the equations

$$\begin{cases} \varepsilon(\widehat{w}_p)_t = i\xi\widehat{w}_p + \dfrac{\varepsilon^p}{(i\xi)^p} \dfrac{\partial^p \hat{f}_2(\xi, t)}{\partial t^p}, \\ \widehat{w}_p(\xi, 0) = \widehat{u}_0(\xi) + \displaystyle\sum_{j=0}^{p-1} \frac{\varepsilon^j}{(i\xi)^{j+1}} \frac{\partial^j \hat{f}_2(\xi, 0)}{\partial t^j}. \end{cases} \tag{12}$$

The Fourier transformed solution (11) is a valid asymptotic expansion when $\varepsilon/|\xi| \ll 1$, *i.e.*, $|\xi| > K\varepsilon$ for $K \gg 1$. It is, then, sufficient, to choose

$$\eta = K\varepsilon, \tag{13}$$

for some constant $K \gg 1$, since we are on the domain $|\xi| \geq \eta$.

We now move to examining what this solution form in frequency space implies about the behavior of the solution in physical space. Let us first transform $\widehat{S}$ from equation (11) back to physical space, so we may examine the effect of this piece on solution w

of equation (9):

$$S(x,t) = \frac{1}{\sqrt{2\pi}}\left(\int_{-\infty}^{-\eta} e^{ix\xi}\widehat{S}(\xi,t)\,d\xi + \int_{+\eta}^{+\infty} e^{ix\xi}\widehat{S}(\xi,t)\,d\xi\right) =$$

$$= \frac{-1}{\sqrt{2\pi}}\sum_{j=0}^{p-1}\varepsilon^j\left(\underbrace{\int_{-\infty}^{-\eta} e^{ix\xi}\,\frac{\partial^j \hat{f}_2(\xi,t)/\partial t^j}{(i\xi)^{j+1}}\,d\xi}_{\text{Integral}\,A1} + \underbrace{\int_{+\eta}^{+\infty} e^{ix\xi}\,\frac{\partial^j \hat{f}_2(\xi,t)/\partial t^j}{(i\xi)^{j+1}}\,d\xi}_{\text{Integral}\,A2}\right).$$

Taking inegral $A2$, for example, we perform a change of variables, substituting ξ' for ξ/η, giving

$$A2 = \int_{-\infty}^{-\eta} e^{ix\xi}\,\frac{\hat{f}_2(\xi,t)}{(i\xi)^{j+1}}\,d\xi = \frac{\eta}{\eta^{j+1}}\int_{+1}^{+\infty} e^{i(\eta x)\,\xi'}\,\frac{\hat{f}_2(\eta\xi',t)}{(i\xi')^{j+1}}\,d\xi'.$$

A similar manipulation can be carried out on integral $A1$. We can now write

(14) $S(x,t) =$

$$= \frac{-\eta}{\sqrt{2\pi}}\sum_{j=0}^{p-1}\frac{\varepsilon^j}{\eta^{j+1}}\left(\int_{-\infty}^{-1} e^{i(\eta x)\,\xi}\,\frac{\partial^j \hat{f}_2(\eta\xi,t)/\partial t^j}{(i\xi)^{j+1}}\,d\xi + \int_{1}^{\infty} e^{i(\eta x)\,\xi}\,\frac{\partial^j \hat{f}_2(\eta\xi,t)/\partial t^j}{(i\xi)^{j+1}}\,d\xi\right)$$

where the prime symbol (′) has been dropped on the ξ for convenience.

In the same way, performing a change of variables on the Fourier representation of $f_2(x,t)$ yields (see (6) and (8)),

$$f_2(x,t) = \frac{1}{\sqrt{2\pi}}\left(\int_{-\infty}^{-\eta} e^{ix\xi}\hat{f}_2(\xi,t)\,d\xi + \int_{+\eta}^{+\infty} e^{ix\xi}\hat{f}_2(\xi,t)\,d\xi\right) = \tag{15}$$

$$= \frac{\eta}{\sqrt{2\pi}}\left(\int_{-\infty}^{-1} e^{i(\eta x)\,\xi}\hat{f}_2(\eta\xi,t)\,d\xi + \int_{+1}^{+\infty} e^{i(\eta x)\,\xi}\hat{f}_2(\eta\xi,t)\,d\xi\right).$$

Comparing $S(x,t)$ in (14) with $f_2(x,t)$ in (15) gives us an estimate for $S(x,t)$ in terms of the forcing $f_2(x,t)$, namely,

$$|S(x,t)| \leqslant \sum_{j=0}^{p-1}\frac{\varepsilon^j}{\eta^{j+1}}\left|\frac{\partial^j f_2(x,t)}{\partial t^j}\right|. \tag{16}$$

This shows that each slow term in the asymptotic expansion $S(x,t)$ is bounded by the behavior of $f_2(x,t)$ and its first $p-1$ time derivatives. The estimate also depends on ε and the choice of η.

We next examine the contribution of the remainder term $\widehat{w}_p$ in (11) to the solution.

Since the forcing function in equations (12) is only of magnitude $\mathcal{O}(\varepsilon^p)$, the more significant contribution from $\widehat{w}_p$ is likely to come from the initial data. Therefore, we focus our attention on the effect of the initial data in (12). Upon transforming equations (12) back to physical space, we see that the form of the physical space equations is that of our original transport equation (4):

$$\varepsilon w_{p_t} = w_{p_x} + \varepsilon^p \int_{-\infty}^{-\infty} \frac{\partial^p \hat{f}_2(\xi, t)}{\partial t^p} e^{x\xi} \, d\xi , \tag{17}$$

with initial data given by

$$w_p(x, 0) = u_0(x) - \frac{1}{\sqrt{2\pi}} \sum_{j=0}^{p-1} \varepsilon^j \cdot$$

$$\cdot \left(\int_{-\infty}^{-\eta} e^{ix\xi} \frac{\partial^j \hat{f}_2(\xi, 0)}{\partial t^j} \frac{1}{(i\xi)^{j+1}} \, d\xi + \int_{+\eta}^{+\infty} e^{ix\xi} \frac{\partial^j \hat{f}_2(\xi, 0)}{\partial t^j} \frac{1}{(i\xi)^{j+1}} \, d\xi \right) = u_0(x) + S(x, 0) .$$

It is then clear that these new initial data also move through our domain at speed t/ε. The difference is that although $u_0(x)$ is compact in space, which implies that after a short period of time, we no longer see the effects of $u_0(x)$, the portion of the initial data arising from $S(x, 0)$ is no longer necessarily compact in space. However, since the inverse transform $f_2(x, t)$ of $\hat{f}_2(\xi, t)$ is known to decay at least like $1/x$ in physical space, this implies that the physical initial data, $u_0(x) + S(x, 0)$, also will decay in space at least like $1/x$, because of our estimates. Using our bound on $S(x, t)$ given in (16), we see immediately that

$$|w_p(x, 0)| \leq |u_0(x)| + |S(x, 0) \leq |u_0(x)| + \underbrace{\sum_{j=0}^{p-1} \frac{\varepsilon^j}{\eta^{j+1}} \left| \frac{\partial^j f_2(x, 0)}{\partial t^j} \right|}_{\text{Constant in time}} \leq |u_0(x)| + \left| \frac{C}{x} \right|$$

for constant C as specified, and for x large.

Suppose that function $u_0(x)$ has support within $x \in [a, b]$. Let us also choose our domain of interest to be the interval $x \in [a, b]$. Recall that the «domain of interest» refers to some fixed, bounded subregion of the infinite domain. Then for all $t > \varepsilon(b - a)$, the effects of $u_0(x)$ have been completely transported out of the domain of interest.

Now, suppose we represent our initial data by the function $U(x)$. The fact that $U(x)$ decays like $1/x$ in space means that if we fix a point in space to observe, a point which lies within the domain of interest, the contribution of the initial data $U(x)$ after time t at point x is given by $U(x + t/\varepsilon)$. The magnitude of $U(x + t/\varepsilon)$ is $\mathcal{O}(\varepsilon/t)$ of the magnitude of $U(x)$ at point x at time zero. Therefore, after only a short time, the effect of the initial data on our solution within the bounded domain of interest will be negligible. After some finite time, the main contribution to solution ω_p within the domain of interest will come from the forcing function, which has been reduced to $\mathcal{O}(\varepsilon^p)$.

In sum, the analysis of equation (9) has shown that the solution to equation (9) can be written

$$w(x, t) = u_0(x + t/\varepsilon) + S_0(x + t/\varepsilon) + S(x, t) + \mathcal{O}(\varepsilon^p),$$

where $S_0(x) = S(x, 0)$. Additionally, within the domain of interest, and for $t > t_0 > 0$ for some t_0, the solution to (9) will be bounded as

$$|w(x, t)| \leq \sum_{j=0}^{p-1} \frac{\varepsilon^j}{\eta^{j+1}} \left| \frac{\partial^j f_2(x, t)}{\partial t^j} \right| + \mathcal{O}(\varepsilon^p). \tag{19}$$

2.2. *Low frequency driven behavior.*

Let us now examine the behavior of v described in (10). The function $\hat{f}_1$ has support on the interval $[-\eta, \eta]$. Therefore the Fourier representation of the corresponding portion of the forcing function in physical space is given by

$$f_1 = \frac{1}{\sqrt{2\pi}} \int_{-\eta}^{\eta} e^{ix\xi} \hat{f}_1(\xi, t)\, d\xi. \tag{20}$$

We re-write the Fourier representation of f_1, letting $\eta = K\varepsilon$ by (13) and then perform a change a variables, letting $\xi' = \xi/\varepsilon$ be the new Fourier space variable. This gives

$$f_1 = \frac{1}{\sqrt{2\pi}} \int_{-K\varepsilon}^{K\varepsilon} e^{ix\xi} \hat{f}_1(\xi, t)\, d\xi =$$

$$= \frac{1}{\sqrt{2\pi}} \int_{-K\varepsilon}^{K\varepsilon} e^{i(\varepsilon x)(\xi/\varepsilon)} \hat{f}_1(\xi, t)\, d\xi = \varepsilon \underbrace{\left(\frac{1}{\sqrt{2\pi}} \int_{-K}^{K} e^{i(\varepsilon x)\xi'} \hat{f}_1(\varepsilon\xi', t)\, d\xi' \right)}_{\tilde{f}_1(\varepsilon x, \varepsilon, t)}.$$

This means that $f_1 = \varepsilon \tilde{f}_1(\varepsilon x, \varepsilon, t)$ is a function of (εx) and ε. For convenience, we suppress the ε variable and write $f_1 = \varepsilon \tilde{f}_1(\varepsilon x, t)$ instead of $f_1 = \varepsilon \tilde{f}_1(\varepsilon x, \varepsilon, t)$. In (10) we make a change of variables, letting $x' = \varepsilon x$, and write

$$v_t = v_{x'} + \tilde{f}_1(x', t), \qquad v(x', 0) = 0. \tag{21}$$

This has exact solution

$$v(x, t) = \int_0^t \tilde{f}(\varepsilon x + t - \tau, \tau)\, d\tau = Q(\varepsilon x, t). \tag{22}$$

We now see that f_1 gives rise to a solution which varies slowly in space, on the scale of $\mathcal{O}(\varepsilon x)$. That is, variation will be observed over a spatial range $x = 1/\varepsilon$. The implication is that the effects of local sources can be seen over very large domains. We see from the solution (22) that even after the forcing function has been shut off in time, *i.e.*, t is large enough so $f(x, t) = 0$, the effect of the forcing term is still brought in through the time integral. Therefore, large space scale solutions persist for all times, even when the source of the large space scale solution has been turned off.

By equations (18) and (22), one now sees that the complete solution to equation (4), represented by

$$u = v + w\,, \tag{23}$$

has a portion which varies on the $\mathcal{O}(x)$ space scale, brought in through w, and a portion which varies on the $\mathcal{O}(\varepsilon x)$ space scale, brought in through v. This slow spatial variation will only be observed over domains where the support of the forcing function is small with respect to the size of the domain of observation. The $\mathcal{O}(x)$ spatial variations will disappear after the forcing function has been shut off in time, but the $\mathcal{O}(\varepsilon x)$ variations will remain throughout all time. As mentioned previously, the fast *time* scale variations are considered to have little impact on the solution since the initial data tend to travel rapidly away from the domain of observation.

Theorem 1 of Section 1 has been proved.

3. – Numerical experiments.

In this section we visualize our results through numerical experiments. We solve the nondimensionalized transport equation of the form

$$\varepsilon u_t = u_x + f(x, t)\,, \qquad t \geqslant 0\,,$$

$$u(x, 0) = u_0\,,$$

on the domain $x \in [-500, 500]$. The forcing function and initial data are chosen to be

Forcing: $f(x, t) = f_1(x, t) + f_2(x, t)\,,$

Initial data: $u_0(x) = 0.0\,,$

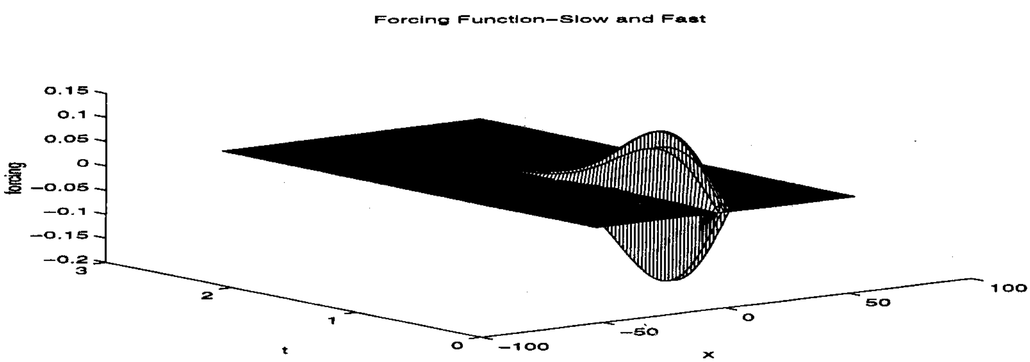

Fig. 1. – Forcing function $f(x, t)$.

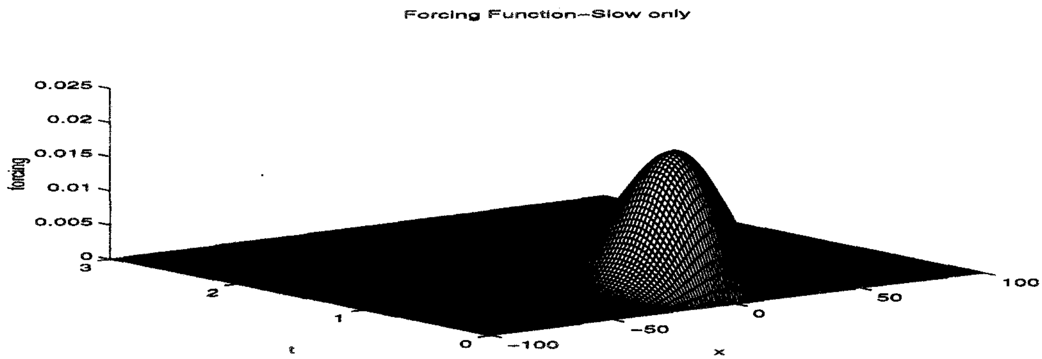

Fig. 2. – Low frequency forcing component $f_1(x, t)$.

where

$$f_1(x, t) = \frac{\sqrt{2}}{20} e^{-x^2/400} \sin(t) e^{-2t^2},$$

$$f_2(x, t) = \sqrt{2}(\cosh(x^2/4) - \sinh(x^2/4))\cos(10x)\sin(t) e^{-2t^2}.$$

The initial data are set to zero since we want to focus on the effects of the forcing function alone. We choose the wave speed to be 100, that is, $\varepsilon = 1/100$. The forcing function is chosen so that it will die away smoothly in space, and both start up and die away smoothly in time. Although the function is not compact mathematically, it can be considered to be compact numerically, since by machine precision values become zero for large x and large t.

Three dimensional mesh plots of the forcing function, along with its low frequency and high frequency components, are shown in figures 1, 2 and 3. The right horizontal

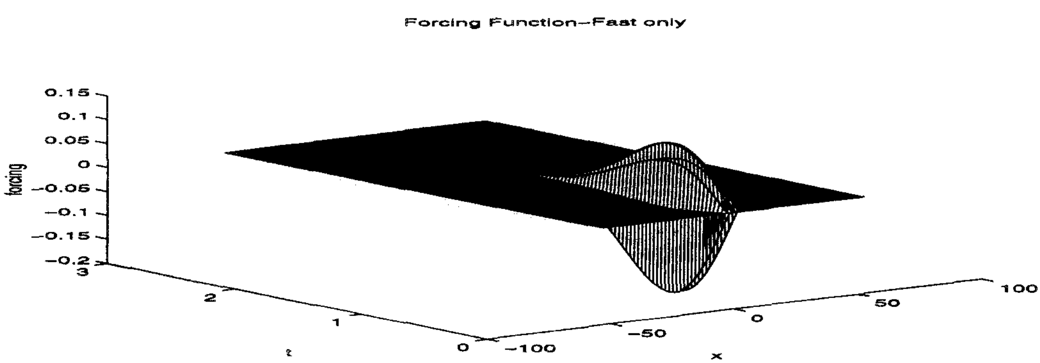

Fig. 3. – High frequency forcing component $f_2(x, t)$.

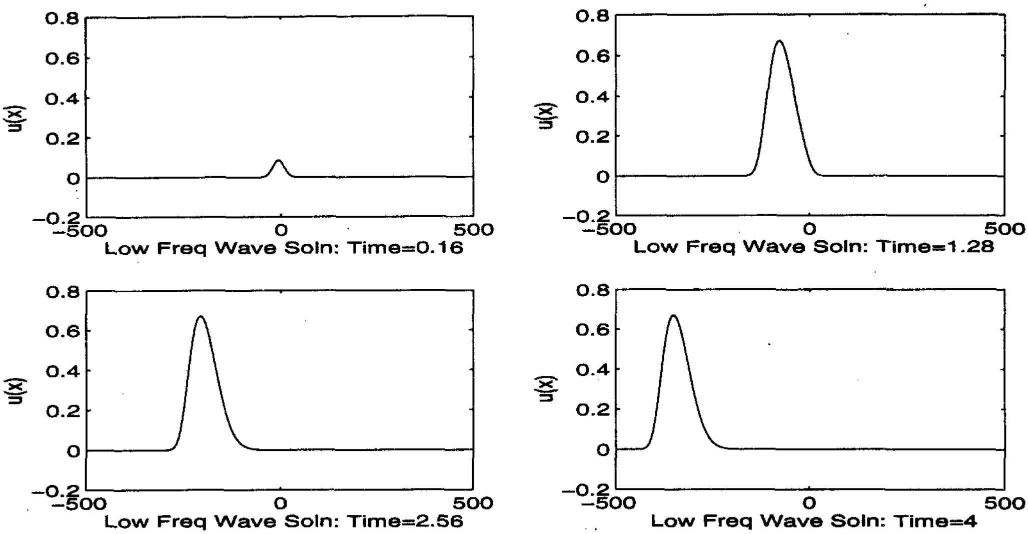

Fig. 4. – Solution profile, $\varepsilon = 0.01$, forcing $f_1(x, t)$.

axis is the spatial axis, and runs from -100 to 100. The left horizontal axis is the time axis, and runs from 0 to 3, The vertical axis is the forcing function height.

We note that since the Fourier transforms of the forcing are given by

$$\hat{f}_1(w, t) = e^{-100w^2} \sin(t)\, e^{-2t^2},$$

$$\hat{f}_2(w, t) = (e^{-(w-10)^2} + e^{-(w+10)^2}) \sin(t)\, e^{-2t^2}$$

it is clear that f_1 will give rise to the long spatial waves, and f_2 will give rise to the short spatial waves.

We employ a method of lines scheme which uses sixth order centered finite differences in space, and a fifth to sixth order adaptive Runge-Kutta method in time. Fortran code MOL1D [4] was run on a Sparc 1 workstation. Numerically, one must be careful when trying to capture both the large and the small spatial scales simulaneously. In order to run a numerical experiment to completion within a reasonable amount of time with the above mentioned hardware and software, we can discretize in space with at most 2000 steps. This means, that over $x \in [-500, 500]$, we can get at best space step $dx = 0.5$. This is sufficient to capture the large scale solutions, but not the small scale ones. In order to capture the small scale solutions, we need at least $dx = 0.01$, which means we need to run our calculation over $x \in [-10, 10]$ instead. However, in this range, the large space scale variation will not be observable.

The solution to this dilemma is to run the two cases separately, one over the large spatial range, and one over the small spatial range. Since solution $u(x, t) = v(x, t) + w(x, t)$ can be split, as in equation (23), where v is driven by f_1 and w is driven by f_2, we separately observe the solutions of $v(x, t)$ and $w(x, t)$ instead.

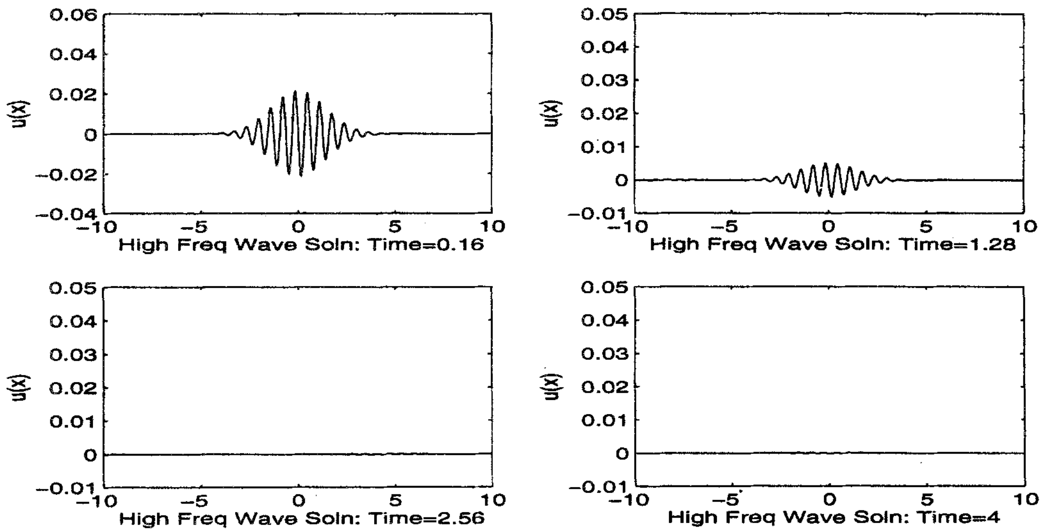

Fig. 5. – Solution profile, $\varepsilon = 0.01$, forcing $f_2(x, t)$.

Experiments were run from time $t = 0$ to $t = 4$. In figures 4 and 5 we view the results of four time snapshots of the experiment, with wave-speed set to 100.

Figure 4 plots the portion of the solution which changes on an $\mathcal{O}(\varepsilon x)$ space scale. In contrast to the high frequency portion of the solution in figure 5, this low frequency portion, while traveling through the domain of interest, clearly does *not* decay away in time, even though the source itself does. This is the $\mathcal{O}(\varepsilon x, t)$ portion of our solution, and is behaving as the mathematics of the previous section predicts.

Figure 5 clearly shows the portion of the solution which changes on an $\mathcal{O}(x)$ space scale. As opposed to the low frequency portion of the solution, this high frequency part dies out in time as the forcing function dies out in time. This is the $S(x, t)$ portion of our solution. There are, of course, no initial data effects to see. The remaining portion of the solution which travels rapidly out of the domain of interest, $S_0(x + t/\varepsilon)$, is small enough in magnitude that it is not discernible with the numerics.

These numerical findings are consistent with the analysis of earlier sections, and that of section (2.2) in particular, where it was predicted that the transport equation solution would vary over large space scales, proportional to the wave speed $1/\varepsilon$.

4. – Conclusions.

An examination, both analytical and numerical, of the transport equation in one space dimension, has been carried out. It is known that when the equation has wave speed on the order of $1/\varepsilon$, slow and fast time scales are introduced. We have seen additionally, that the presence of a localized forcing function will give rise to portions of the solution which vary over larger space scales which persist for all times, even when the forcing function has been shut off. If the domain of observation is smaller than $1/\varepsilon$, these variations will not be seen.

Having analyzed the solutions of the one-dimensional wave equation (via the one-dimensional transport equation) in Section 2, we intend, in a future work, to advance to an analysis of the wave equation in two and three dimensions. It is surmised that the results can be pushed through, virtually in tact, to higher dimensions.

Additionally, it might be of interest to perform an analysis of the higher-dimensional transport equation, which is used in the modeling of various physical phenomena such as neutron diffusion and radiation transfer. In this case, it is not so clear that the extension to higher dimensions will be so straightforward, either analytically or computationally. This remains to be seen.

Acknowledgements. The author would like to thank Prof. HEINZ-OTTO KREISS of the University of California, Los Angeles, Mathematics Departments for several helpful discussions.

REFERENCES

[1] R. N. BRACEWELL, *The Fourier Transform and its Applications*, Second Edition, McGraw-Hill Book Company (1978).

[2] G. BROWNING - H.-O. KREISS, *Problems with different time scales for nonlinear partial differential equations*, SIAM J. Appl. Math., 42 (1982), pp. 704-718.

[3] L. G. DE PILLIS, *Far-field behavior of slightly compressible flow*, Computational and Applied Mathematics Report, no. 93-15, Department of Mathematics, UCLA, Los Angles (1993).

[4] J. M. HYMAN, *Software: MOL1D Fortran Subroutine Library*, Los Alamos Laboratory, Los Alamos, New Mexico (1976).

[5] S. KLAINERMAN - A. MAJDA, *Compressible and incompressible fluids*, Comm. Pure Appl. Math., **35** (1982), pp. 629-651.

[6] H.-O. KREISS, *Problems with different time scales for ordinary differential equations*, SIAM J. Numer. Anal., **16** (1979), pp. 980-998.

[7] H.-O. KREISS, *Problems with different time scales for partial differential equations*, Comm. Pure Appl. Math., **33** (1980), pp. 399-439.

[8] H.-O. KREISS, *Problems with Different Time Scales*, Academic Press, Inc. (1985).

[9] H.-O. KREISS - J. LORENZ, *Initial-Boundary Value Problems and the Navier Stokes Equations*, Academic Press, Incx. (1989).

[10] H.-O. KREISS - J. LORENZ - M. J. NAUGHTON, *Convergence of the solutions of the compressible to the incompressible Navier-Stokes equations*, Adv. Appl. Math., **12** (1991), pp. 187-214.